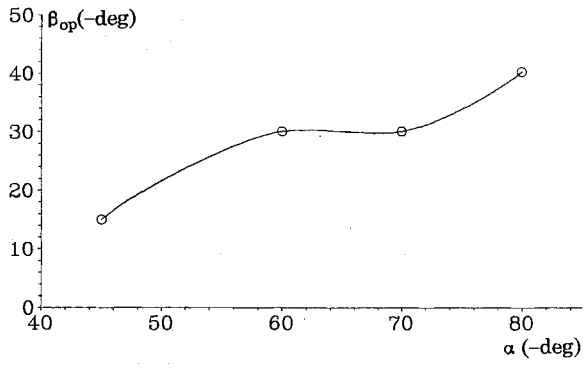

Fig. 3 Relationship of α and β_{op}.

Results and Discussion

Figure 1 gives the cross flow velocities at the duct exit at 80-deg angle of attack. It is observed that the cross flow velocity becomes larger as the angle of attack α increases up to 80 deg. The flowfield is badly distorted, and a strong vortex exists inside the inlet. The use of the variable lip affects the entrance air flow. With a gradual increase of β, two effects occur: 1) the angle of attack seems to reduce, and 2) a door with the same effect as an auxiliary air intake door (AAID) exists behind this lip because of its rotation, and allows air flow with a high kinetic energy into the diffuser. Figure 1 also shows the reduction of the swirl flow at 80-deg angle of attack when β is 40 deg. The test results show the variations of swirl coefficient SC_{60}, entrance air flow flux Q, average total pressure coefficient η_σ, and pressure distortion index DC_{60} with the angle of the lip β at 45-, 60-, 70-, and 80-deg angles of attack. From Fig. 2 it is observed that there is a minimum value of SC_{60} for every curve. The SC_{60} can be reduced by about 40% when α is 80 deg and β is 40 deg. An increase in the entrance air flow is obtained at high angles of attack. Q is increased by about 22% at α = 80 deg and β = 40 deg. With the variable lip, the total pressure loss and its distortion are reduced considerably. For an α of 80 deg and a β of 40 deg, η_σ increases by 40% and DC_{60} decreases by almost 43%. There is an optimum angle of the variable lip β_{op} for every angle of attack where a maximum improvement in flow performance is obtained. β_{op} is a function of α, as shown in Fig. 3. Although more work is needed for compressible flow, the relationship of α and β_{op} is of great value for automatic control of intake swirl.

Conclusions

The main conclusions drawn from the preceding are the following. 1) The variable lip technique improves flow properties in an S-shaped duct at the high angle of attack. A valuable relationship between α and β_{op} is established in the paper. 2) The variable lip has two effects: a) a reduction of the effective angle of attack, and b) an effect similar to that of an AAID.

References

[1]Stocks, C. P., and Bissinger, N. C., "The Design and the Development of the Tornado Engine Air Intake," AGARD Symposium on Aerodynamics of Power Plant Installation, Paper 10, May 1981.

[2]Guo, R. W., and Seddon, J., "The Swirl in an S-Duct of Typical Air Intake Proportions," *Aeronautical Quarterly*, Vol. 32, Pt. 2, May 1983, pp. 99–129.

[3]Guo, R. W., and Seddon, J., "Swirl Characteristics of an S-shaped Air Intake with both Horizontal and Vertical Offsets," *Aeronautical Quarterly*, Vol. 32, Pt. 2, May 1983, pp. 130–146.

[4]Seddon, J., "Understanding and Countering the Swirl in an S-Duct, Testing on the Sensitivity of Swirl to Fence," *Aeronautical Journal*, Vol. 88, No. 874, 1984, pp. 117–127.

[5]Vakili, A. D., Wu, J. M., Liver, P., and Brat, M. K., "Flow Control in a Diffusing S-Duct," AIAA Paper 85-0524, March 1985.

[6]Weng, P. F., and Guo, R. W., "New Method of Swirl Control in a Diffusing S-Duct," *AIAA Journal*, Vol. 30, No. 7, 1992, pp. 1918, 1919.

Relationship Between Stokes Number and Intrinsic Frequencies in Particle-Laden Flows

S. K. Aggarwal*
University of Illinois at Chicago, Chicago, Illinois 60680

Introduction

A KEY parameter characterizing particle dispersion in turbulent flows is the Stokes number, defined as the ratio of the particle response time (t_p) to the appropriate time scale of turbulence or flow time (t_f). While the particle response time is generally taken as $t_p = \rho_p d_p^2/(18\mu)$, assuming the Stokes drag law, the choice of a proper flow time is somewhat ambiguous because of the existence of several time scales in a turbulent shear flow. Results from both laboratory experiments[1–4] and numerical simulations[5,6] indicate that the flow dynamics as well as the particle dispersion behavior in the near region of a shear flow are controlled by large-scale coherent structures. Naturally, a proper flow time for defining the Stokes number should be based on a flow time associated with the dynamics of large structures. The latter time is generally defined from the global length and velocity scales of the structures. However, this definition is somewhat ambiguous in situations when the shear flow under consideration lacks an intrinsic length scale. For example, using the initial momentum thickness in a developing planar shear layer would not yield the correct flow time scale. In such cases, one may be able to use the intrinsic time scale of the unsteady flow for defining the Stokes number. The objective of this note is to propose, based on the results of numerical simulations, that using the dominant frequency of the shear flow can yield the proper flow time scale for defining the particle Stokes number. Results presented on particle dispersion indicate that the dominant frequency is the fundamental frequency for a planar shear layer, and the preferred mode frequency for an axisymmetric jet flow. Several experimental results from the literature[1–4] are used to further substantiate the hypothesis.

It is recognized that relating the flow time scales to the dominant frequencies in a shear flow is not a novel concept. In fact, there exists a large body of experimental and theoretical work[9,10] focusing entirely on identifying the dominant frequencies in different shear flows. However, none of the studies concerning particle dispersion in large coherent structures has used the dominant frequency to define the particle Stokes number.

Results and Discussion

The dynamics of large-scale vortex structures in the developing planar shear layer and axisymmetric jet are simulated by employing a finite-difference method based on the monotone integrated large eddy simulation (MILES) algorithm.[7] The dynamics of solid particles injected into the shear flows is simulated by solving the standard particle equations by a Runge-Kutta procedure. Further details are provided in a separate study.[8] The gas-phase algorithm employs a fourth-order accurate, flux-corrected transport method with a directional time-splitting technique with appropriate inflow and outflow boundary conditions, and is shown to reproduce the large-scale features of a variety of flows that are observed in the laboratory experiments. Although no explicit subgrid model is used, the algorithm is demonstrated[7] to incorporate a built-in subgrid model. Moreover, because the present study considers the influence of large coherent structures on particle dispersion in the initial region of two shear flows, the algorithm is expected to be sufficiently accurate for the stated objective.

Received March 23, 1993; revision received Nov. 16, 1993; accepted for publication Dec. 18, 1993.

*Associate Professor, Department of Mechanical Engineering. Associate Fellow AIAA.

First, the dispersion results are presented for particles injected into the initial region of a jet flow. The air jet is issuing out at a velocity of 200.0 m/s from a nozzle of diameter 1.4 cm. A portion of the nozzle, 1.64 cm in length, is placed inside the computational domain. This allows the pressure at the inflow region to respond smoothly to fluid accelerations downstream, thus enabling the instability to evolve naturally in the calculations. The computational domain is 57.2 cm in the streamwise direction and 6.8 cm in the radial direction. A nonuniform grid is used with 422 × 122 points in the streamwise and radial direction, respectively. The temporal step size used is 10^{-7} s, yielding a Courant number of 0.5. The large eddy simulation reproduces the large- scale features of the jet flow observed in the experiments. This includes the Strouhal numbers for the shear layer rollup and jet-preferred-mode frequencies, the spatial distributions of merging locations, and the shear layer growth rate. For example, the predicted shear layer instability frequency, $S_{\theta 0} = f_{\theta 0}/U_0 = 0.014$, is in the expected range of laboratory experiments.[9] In addition, the results on particle dispersion were established to be independent of the temporal step size and the number of particles used for statistical information.[8] For the dispersion results, the near jet region is considered, extending 9.00 cm (about six jet diameters) in the axial direction; the nature of coherent structures is much better understood in this region and the structures tend to become three-dimensional further downstream.[3]

The transverse dispersion of particles, due to their interaction with large vortex structures, is quantified by a dispersion function defined as

$$D(t, N) = \left\{ \sum_{i=1}^{\infty} [X_i(t) - X_{i,o}]^2 / N \right\}^{1/2} \quad (1)$$

where $X_i(t)$ is the transverse location of particle i at time t, X_{io} is the corresponding starting location for the particle, and $N(t)$ is the number of particles in the flow under consideration. The dispersion function is obtained by following the Lagrangian motion of a large number of particles in the shear layer. Figure 1 shows the dispersion function vs time for particles of different diameters (d_p) injected into the shear layer of the axisymmetric jet. The dispersion function increases with time, as the particles are convected radially outward by the coherent structures and more particles are injected into the flow. The data in the figure can be cross plotted to display the dependence of dispersion function with particle diameter, shown in Fig. 2. For each size, 1100 particles are used in the dispersion calculation. The plot for particle density $\rho_p = 1.0$ gm/cm^3 represents the base case. Figure 2 clearly indicates the selective nature of the dispersion process and the range of particle sizes where the particle radial dispersion exceeds the gas-phase dispersion. The result is in agreement, at least qualitatively, with the experimental and numerical results of previous studies.[1–6] The focus of this paper is to further study the dependence of particle dispersion on the Stokes number, and to re-examine the flow time scales used in defining the Stokes number.

As discussed earlier, the flow time (t_f) used in defining the Stokes number is generally based on the global length and velocity

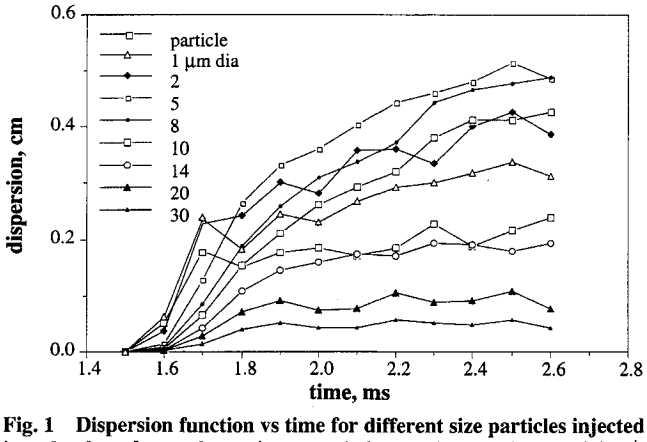

Fig. 1 Dispersion function vs time for different size particles injected into the shear layer of an axisymmetric jet; the jet velocity is 200.0 m/s and the jet diameter = 1.4 cm.

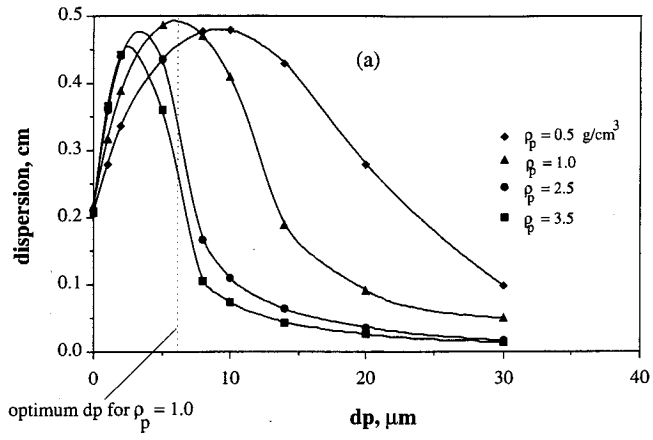

Fig. 2a Dispersion function vs particle diameter for different particle densities.

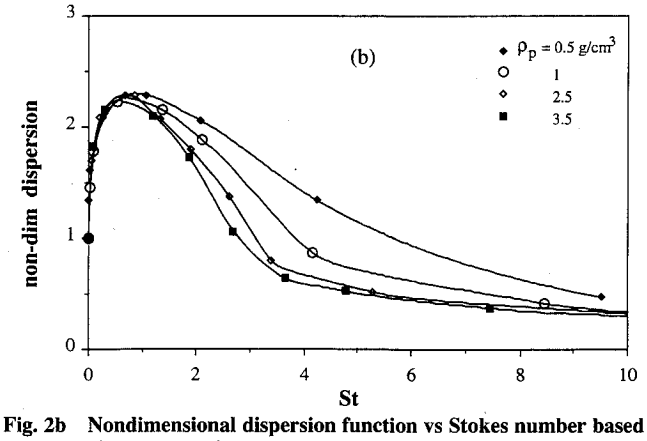

Fig. 2b Nondimensional dispersion function vs Stokes number based on the preferred mode frequency for the jet flow.

scales of the large-scale motions. For a jet flow, t_f is usually defined by the ratio of jet diameter to jet velocity. However, both our numerical results and physical considerations suggest that the flow time can also be based on the preferred mode frequency (f_p) of the jet. As discussed by Hussain and Zaman,[10] the preferred mode is the most dominant of all large-scale coherent structures in an unperturbed circular jet, i.e., an axisymmetric disturbance receives maximum amplification at the preferred mode frequency. For the results in Figs. 1 and 2, the Stokes number (St_1) based on $t_p = \rho_p d_p^2/(18\,\mu)$ and $t_f = 1/f_p$ is given in Table 1. Also shown is the Stokes number (St_2) based on a flow time scale defined as $t_f = d_j/u_j$. It is interesting to note that the two Stokes numbers differ by a factor of 0.49 ($St_1/St_2 = 0.49$) which is the preferred mode Strouhal number obtained from the numerical simulations. Although the results cannot be considered conclusive, t_f based on the preferred mode appears to provide as good a correlation between particle dispersion and Stokes number as that based on the ratio d_j/u_j. For example, numerical and experimental results[6] indicate that the particle dispersion maximizes at a Stokes number of about unity. This is confirmed here by the Stokes number based on the preferred mode frequency; for the base case ($\rho_p = 1.0$) the optimum diameter for maximum dispersion is 7.0 μm which corresponds to $St_1 = 1.04$. A further validation is provided in Fig. 2b, where the dispersion function, normalized by the corresponding value for the gas particles, is plotted vs the Stokes number (St_1) based on the preferred mode frequency. At lower Stokes numbers ($St_1 < 2.0$), the dispersion function is well-correlated with the Stokes number. At higher Stokes numbers, the correlation displays a weak dependence on particle density (ρ_p) , which is due to the errors associated with the use of the Stokes drag assumption in defining the particle response time. As ρ_p is reduced ($\rho_p = 0.5$), its effect on the correlation becomes somewhat stronger, implying that the forces due to flow nonuniformity, particle acceleration, Basset effects, etc. may not be negligible at reduced particle density. It is also important to note that the results at a different value of jet initial velocity or diameter will lead to essentially the same conclusion, as

the ratio of the two flow times, i.e., the preferred mode Strouhal number, is mostly independent of d_j and u_j. In fact, the preferred mode Strouhal number, according to several theoretical and experimental studies,[10] lies in the range 0.35-0.50, implying that St_2 can differ from St_1 by a factor of 2–3.

Similar results are now presented for particles injected into a planar shear layer formed by two coflowing streams past a splitter plate. Employing the same methodology as was used for the axisymmetric jet, the dispersion function is obtained as a function of the particle size. Figure 3a shows the variation of dispersion function with particle diameter for different values of particle density, whereas Fig. 3b shows the nondimensional function vs the Stokes number. It is clearly seen that, like the jet flow, the dispersion function maximizes at a certain particle diameter, which is a function of the particle density. However, unlike the jet flow, the use of an appropriate flow time scale for calculating the Stokes number is somewhat ambiguous for the planar shear layer, because the shear layer does not have a fundamental length scale, other than the initial momentum thickness (θ). Using θ and $\Delta U = U_1 - U_2$, where U_1 and U_2 are, respectively, the velocities of fast and slow streams, one would get totally unacceptable values for the Stokes number. For example, this would yield a Stokes number of 253 for a particle diameter of 5 μm. Another possibility is to define $t_f = L/\Delta U$, where L is the length scale of large-scale structures. Chein and Chung[5] used an average width of large-scale structures to represent L, which is also somewhat ambiguous as the shear layer grows downstream due to vortex mergings. Our results indicate that t_f can also be obtained from the dominant frequency associated with the large scale structures. Both numerical simulations and experiments indicate that the dominant frequency in the shear layer is the natural instability frequency. In the present study, this frequency was calculated from the spectral analysis of the axial velocity and was found to be in agreement with the experiment values. Using this frequency yields a Stokes number of 0.45 for a particle diameter of 5 μm. A further validation is provided by plotting nondimensional dispersion function vs Stokes number (based on the natural instability frequency) in Fig. 3b. We also estimated a length scale associated with the large structures directly from the vorticity contour and the shear layer thickness plots. Based on the streamwise evolution of mean velocity profiles, the shear layer thickness at an axial location of 7.0 cm, which is approximately the second vortex-merging location, was found to be about 1.6 cm. This yields a Stokes number of 0.53, which is reasonably close to a value of 0.49, obtained from the spectral information. Our recommendation, therefore, is that using the dominant frequency in the shear layer is a reasonable way to calculate the particle Stokes number.

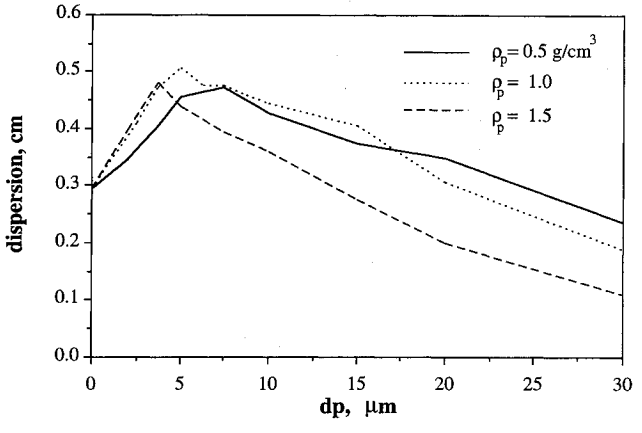

Fig. 3a Dispersion function versus particle diameter for different particle densities.

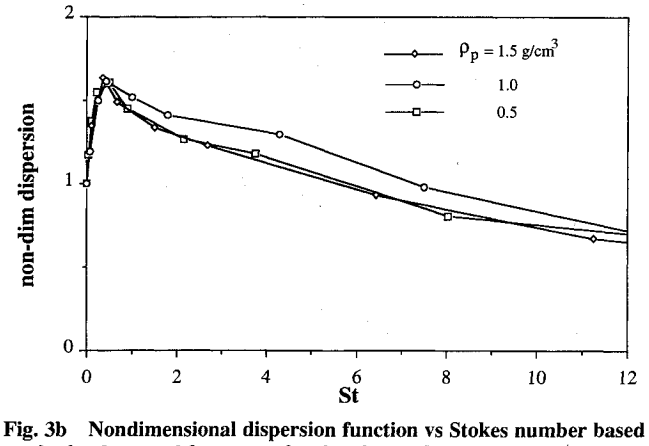

Fig. 3b Nondimensional dispersion function vs Stokes number based on the fundamental frequency for the planar shear layer.

Table 1 Values of two Stokes numbers for representative particle diameters

d_p,μm	St_1	St_2	d_p,μm	St_1	St_2
2	0.08	0.16	12	3.06	6.25
5	0.53	1.08	14	4.17	8.51
7	1.04	2.12	30	19.13	39.05
8	1.36	2.78	50	53.15	108.50

Further Validation Using Experimental Data

Finally, the results of recent experimental studies[1–4] are used to support the hypothesis suggested in this paper. Lazaro and Lasheras[1,2] present experimental results for the dispersion of water droplets in a developing planar shear layer. According to their results, the droplets in the size range 21–35 μm exhibit the maximum dispersion. Following our recommendation, i.e., using the fundamental frequency reported in the experimental study, this corresponds to a Stokes number range of 0.18–0.5. The numerical results presented here indicate a Stokes number of 0.49 corresponding to the maximum droplet dispersion in the shear layer. Additional experimental work on particle dispersion in a planar shear layer is reported by Hishida et. al.[4] They observed enhanced dispersion for 42.0-μm glass particles. Again, following the preceding hypothesis, the flow time calculated from the dominant frequency reported in the experiments yields a Stokes number of 1.28. It should be noted, however, that the minimum particle size considered in the experiments is 42.0 μm; it is quite conceivable that the maximum dispersion may have occurred for smaller particles, i.e., at a lower Stokes number. Longmire and Eaton[3] report an experimental investigation of the effect of vortex ring structures on particle dispersion in the near jet flow region, and conclude that the particle dispersion is controlled not by diffusion but convection by large vortex structures. They employ the average vortex-convection velocity (one-half the jet velocity) but a range of vortex length scales, yielding the Stokes number in the range of 7.2–29. Based on their reported preferred mode frequency, as recommended in this paper, the Stokes number would be 7.6, which is somewhat higher than expected but can be explained by the fact that the particle injection velocity is about one-half the jet velocity in their experiment. As discussed in a separate study,[8] the range of Stokes numbers for enhanced particle dispersion can be significantly increased by reducing the particle injection velocity relative to the jet velocity. The important conclusion, therefore, is that the intrinsic frequency of the shear layer can be used for calculating the Stokes number in a variety of particle-laden shear flows.

In conclusion, it is hypothesized, based on the numerical results, that 1) a proper flow time scale for defining the Stokes number can be related to the dominant frequency associated with the large-scale vortex structures that determine the particle dispersion behavior, and 2) the dominant frequency corresponds to the fundamental instability frequency for the planar shear layer, and the jet preferred mode frequency, for the axisymmetric jet. Results of three different experimental studies on particle dispersion are used to support the hypothesis.

Acknowledgments

This work has been supported by the Air Force Office of Scientific Research through the Wright Laboratory of Wright-Patterson Air Force Base, with Julian M. Tishkoff as the Program Manager. The calculations were performed on Cray Y-MP at the Pittsburgh

Supercomputer Center. Many stimulating discussions with K. Kailasanath and F. Grinstein, both at Naval Research Laboratory, are highly appreciated.

References

[1]Lazaro, B. J., and Lasheras, J. C., "Particle Dispersion in the Developing Free Shear Layer. Pt. 1. Unforced Flow," *Journal of Fluid Mechanics*, Vol. 235, 1992, pp. 143–178.

[2]Lazaro, B. J., and Lasheras, J. C., "Particle Dispersion in the Developing Free Shear Layer. Pt. 2. Forced Flow," *Journal of Fluid Mechanics*, Vol. 235, 1992, pp. 179–221.

[3]Longmire, E. K., and Eaton, J. K., "Structure of a Particle-Laden Jet," *Journal of Fluid Mechanics*, Vol. 236, 1992, pp. 217–257.

[4]Hishida, K., Ando, A., and Maeda, M., "Experiments on Particle Dispersion in a Turbulent Mixing Layer," *International Journal of Multiphase Flow*, Vol. 18, No. 2, 1992, pp. 181–194.

[5]Chein, R., and Chung, J. N., "Effects of Vortex Pairing on Particle Dispersion in Turbulent Shear Flows," *International Journal of Multiphase Flow*, Vol. 13, No. 2, 1987, pp. 785–802.

[6]Crowe, C. T., Chung, J. N., and Trout, T. R., "Particle Mixing in Free Shear Flows," *Progress in Energy and Combustion Science*, Vol. 14, No. 3, 1988, pp. 171–194.

[7]Boris, J. P., Grinstein, F. F., Oran, E. S., and Kolbe, R. L., "New Insights into Large Eddy Simulation, Naval Research Laboratory," Naval Research Lab., NRL/MR/4400-92-6979, Washington, DC, 1992.

[8]Aggarwal, S. K., Uttuppan, J., Grinstein, F. F., and Kailasanath, K., "Particle Dispersion in a Transitional Axisymmetric Jet: A Numerical Simulation," AIAA Paper 93-0105, Jan. 1993.

[9]Hussain, Z. D., and Hussain, A. K. M. F., "Natural Instability of Free Shear Layers," *AIAA Journal*, Vol. 21, No. 11, 1983, pp. 1512–1517.

[10]Hussain, A. K. M. F., and Zaman, K. B. M. Q., "The 'Preferred Mode' of the Axisymmetric Jet," *Journal of Fluid Mechanics*, Vol. 110, 1981, pp. 39–71.

Geometry of Thin Liquid Sheet Flows

Donald L. Chubb* and Frederick D. Calfo†
NASA Lewis Research Center, Cleveland, Ohio 44135
Marc W. McConley‡
Princeton University, Princeton, New Jersey 08544
and
Matthew S. McMaster§ and Abdollah A. Afjeh¶
University of Toledo, Toledo, Ohio 43606

Introduction

INCOMPRESSIBLE, thin-sheet flows have been of research interest for many years. Those studies were mainly concerned with the stability of the flow in a surrounding gas. Squire[1] was the first to carry out a linear, inviscid stability analysis of sheet flow in air and compare the results with experiment. Dombrowski and Fraser[2] did an experimental study of the disintegration of sheet flows using several viscous liquids. They also detected the formation of holes in their sheet flows. Hagerty and Shea[3] carried out an inviscid stability analysis and calculated growth rates for the instability. They compared their calculated growth rates with experimental values. Taylor[4–6] studied extensively the stability of thin liquid sheets both theoretically and experimentally. He showed that thin sheets in a vacuum are stable. Brown[7] experimentally investigated thin liquid sheet flows as a method of application of thin films. Clark and Dombrowski[8] carried out a second-order stability analysis for inviscid sheet flows. Lin[9] introduced viscosity into the linear stability analysis of thin sheet flows in vacuum. Mansour and Chigier[10] conducted an experimental study of the breakup of a sheet flow surrounded by high-speed air. Lin et al.[11] did a linear stability analysis that included viscosity and a surrounding gas. Rangel and Sirignano[12] carried out both a linear and nonlinear inviscid stability analysis that applies for any density ratio between the sheet liquid and the surrounding gas.

Now there is renewed interest in sheet flows because of their possible application as low mass radiating surfaces.[13,14] The objective of this study is to investigate the fluid dynamics of sheet flows that are of interest for a space radiator system. Analytical expressions that govern the sheet geometry are compared with experimental results. Since a space radiator will operate in a vacuum, the analysis does not include any drag force on the sheet flow.

Theory

Sheet Thickness and Sheet Length/Sheet Width Scaling

A sketch of the flow geometry of a thin liquid sheet is shown in Fig. 1. Surface tension forces at the two edges of the sheet push the edges toward the z axis. As a result, as the flow moves in the z direction, the edge cross-sectional area A_c grows. To satisfy mass continuity, the edges approach each other and finally meet at the point $z = L$.

If sheet flow is to be utilized as a space radiator, then the dependence of the sheet length to initial width ratio L/W and sheet thickness τ on the flow conditions must be known. In this section the L/W dependence on the Weber number We will be determined. Also, since all experiments have been performed in the Earth's gravity field, the L/W and τ dependence on a constant gravity force will be included.

The surface tension force acting on the sheet edge in the x direction is given by the following[6,15]:

$$dF_x = 2\sigma\, dz \tag{1}$$

The significance of this result is that it is independent of the cross-sectional shape of the sheet. It applies as long as the edge cross section has infinite slope ($s'' \to \infty$) at the edge ($x = 0$) and zero slope ($s' = 0$) where it joins the constant thickness region ($x = r$). Combining Eq. (1) with the x direction momentum equation yields the following result for the edge velocity in the x direction[6,15]:

$$u_e = \sqrt{\frac{2\sigma}{\rho\tau}} \tag{2}$$

The velocity u_e is the velocity that a free edge of a thin liquid sheet will move regardless of the edge shape. Taylor[6] derived this result earlier without considering the cross-sectional shape of the edge. This is also the phase velocity c_{asy} of the antisymmetrical wave that can exist on a plane sheet.[5,6] It is easily shown[15] that for long sheets ($L/W > 1$) the sheet edge and stationary antisymmetrical waves (lines of constant phase) will be approximately parallel. Experimentally, these waves are observed as they have also been observed in other experiments.[3,6,10]

Equation (2) gives the sheet edge velocity u_e. With this result and the continuity equation, analytical expressions for $\tau(z)$, $x(z)$, and L/W can be developed.[15] In that derivation it is assumed that the flow velocity remains entirely in the z direction until it reaches the edge and that the gravitational force is in the z direction. With these assumptions the following result is obtained for the sheet shape:

$$\frac{2x}{W} = 1 - \frac{2}{3} Fr\sqrt{8/We}\left[\left(1 + \frac{2}{Fr}\frac{z}{W}\right)^{3/4} - 1\right] \tag{3}$$

where the Weber number We, which is the ratio of the dynamic pressure to the surface tension pressure, and the Froude number

Received July 6, 1993; revision received Dec. 22, 1993; accepted for publication Dec. 23, 1993.

*Research Engineer, Photovoltaics Branch. Member AIAA.
†Research Engineer, Aerospace Engineering Branch.
‡Student; currently Graduate Student, Massachusetts Institute of Technology, Department of Aeronautical Engineering.
§Graduate Student; currently at Virtual Engineering, St. Clair Shores, MI.
¶Associate Professor, Department of Mechanical Engineering. Member AIAA.